LA-6362-MS
Informal Report

c.3

CIC-14 REPORT COLLECTION
REPRODUCTION
COPY

UC-21
Reporting Date: May 1976
Issued: June 1976

Lithium Flow on the Inside of a Spherical Fusion-Reactor Cavity

by

I. O. Bohachevsky
L. A. Booth
J. F. Hafer

LOS ALAMOS NATIONAL LABORATORY
3 9338 00322 8839

los alamos
scientific laboratory
of the University of California
LOS ALAMOS, NEW MEXICO 87545

An Affirmative Action/Equal Opportunity Employer

UNITED STATES
ENERGY RESEARCH AND DEVELOPMENT ADMINISTRATION
CONTRACT W-7405-ENG. 36

Printed in the United States of America. Available from
National Technical Information Service
U.S. Department of Commerce
5285 Port Royal Road
Springfield, VA 22161
Price: Printed Copy $3.50 Microfiche $2.25

This report was prepared as an account of work sponsored by the United States Government. Neither the United States nor the United States Energy Research and Development Administration, nor any of their employees, nor any of their contractors, subcontractors, or their employees, makes any warranty, express or implied, or assumes any legal liability or responsibility for the accuracy, completeness, or usefulness of any information, apparatus, product, or process disclosed, or represents that its use would not infringe privately owned rights.

LITHIUM FLOW ON THE INSIDE OF A SPHERICAL FUSION-REACTOR CAVITY

by

I. O. Bohachevsky, L. A. Booth, and J. F. Hafer

ABSTRACT

A model is described for steady-state liquid-lithium flow on the inside of a spherical reactor cavity. The governing equations are derived and discussed together with the physical assumptions implicit in the formulation of the problem. Solutions are determined for different distributions and rates of mass supply from the outside through the porous wall to the inside of the cavity. The self-consistency of the model is demonstrated, and from computed flows it is concluded that inside a sphere of 1.5-m radius a liquid layer several millimeters thick can be maintained easily with a circulating flow of only a few kilograms per second. The thickness of the layer can be made nearly uniform over most of the sphere with relatively simple mass-supply distributions. The need for transient stability analysis is pointed out.

LOS ALAMOS NATL. LAB. LIBS.
3 9338 00322 8839

I. INTRODUCTION

The conceptual design of laser fusion reactors is based on the supposition that a sufficient amount of laser energy will be deposited in the fuel pellet (deuterium-tritium) to initiate thermonuclear reaction. The reaction will be terminated by the pellet expansion, but not before a significant quantity of thermonuclear neutrons and other emissions is generated. The neutrons will be absorbed in a lithium blanket in which their kinetic energy is converted into thermal; the remaining products of the pellet microexplosion, consisting of photons, alpha particles, and plasma debris, will be, in most part, stopped by the first wall of the

reactor cavity. To ensure a long life for the reactor (dictated by economic considerations) the first wall must be protected from the damage inflicted by these microexplosion products.

In the case of a solid first wall, several protection methods have been suggested. Among them are protection with a thin film of liquid lithium, the wetted-wall concept;[1,2] with a magnetic field, the magnetically protected concept;[3] or with a layer of solid carbon, the dry-wall concept.[4] Each of these approaches has its merits and demerits. The pellet burn characteristics and the interaction of reaction products with wall materials must be known in greater detail before an optimal design concept can be selected. In the meantime, the technical feasibility of different alternatives should be explored.

Various aspects of the wetted-wall concept have been investigated in considerable detail;[1,2] however, in these studies, the flow of liquid lithium on the inside of the sphere was not modeled in sufficient detail, and the analysis has been found to be deficient in the treatment of the viscous drag and of the effect of spherical geometry. In the present report we will formulate and justify a model for a thin film of liquid flowing under the action of gravity, discuss some special properties of the governing equations, and present results describing the flow. We will find that the present analysis, in general, validates the observations made in Ref. 1.

II. FLOW MODEL

A. General Description

The configuration of the liquid-lithium film is shown in Fig. 1 together with the coordinate θ used to describe the flow. The physical problem is stated as follows. Liquid lithium is forced through the porous wall of a spherical reactor cavity at a rate of $m_s \cdot g/cm^2 \cdot s$, collects into a layer of thickness δ on the inside of the sphere, flows downward along the wall (positive θ direction) under the action of gravity, and drains through an opening at the bottom, which also serves as an exhaust for evaporated lithium mixed with the remnants of the pellet microexplosion. The operation of this type of reactor is described in greater detail in Ref.

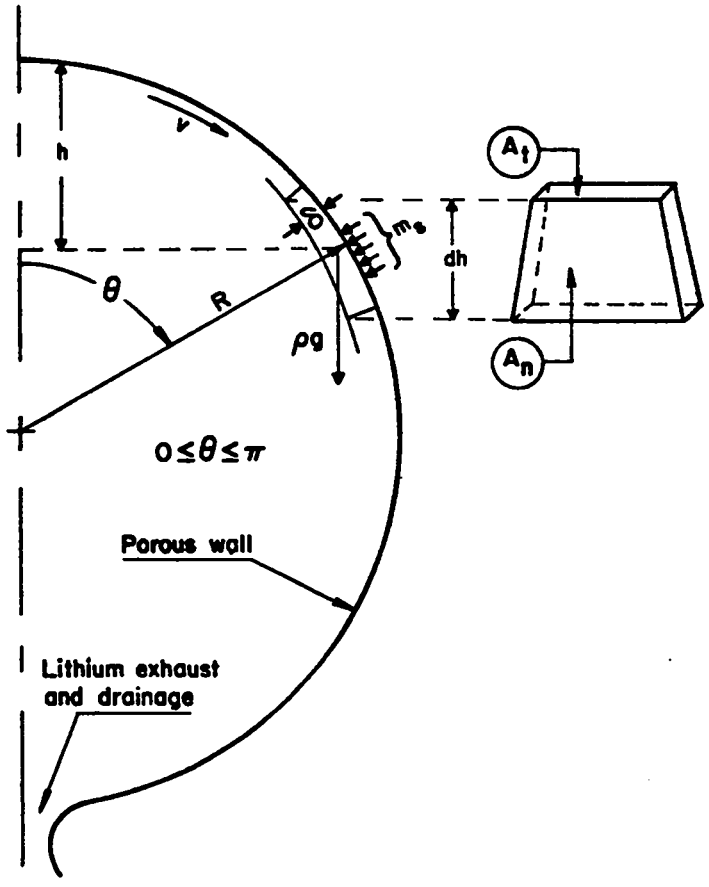

Fig. 1.
Flow configuration.

1. We wish to determine the variations in tangential flow velocity, v, and layer thickness, δ, with the position on the sphere, θ.

Before proceeding, we examine if the above postulated flow is realistic, i.e., whether lithium will adhere to the reactor wall and have enough cohesion to support itself. According to Ref. 5, purified lithium will adhere to ("wet") stainless steel above 625°K or 675°K and impure lithium above 760°K; later investigations,[6] however, determined that the wettability of stainless steel by lithium is improved by small additions of oxygen or nitrogen. Reference 7 indicates that liquid lithium will wet copper. Hence materials and temperature ranges exist for which an adhering film can be maintained; this topic is discussed more extensively in Refs. 6 and 7.

To estimate the maximum layer thickness δ_m that can be supported by adhesive and cohesive forces, we utilize the phenomenon of negative pressure, i.e., the tensile strength of liquid. This phenomenon is well established;[8] however, the numerical values published vary greatly depending on the method of determination. For example, the values of negative pressure for water in Ref. 8, Table 2n-1, range from 2.80×10^8 dyne/cm^2 to 2×10^5 dyne/cm^2, and the value listed for mercury is 4.29×10^8 dyne/cm^2. On the basis of such information, we make a conservative assumption that the tensile strength of liquid lithium, σ, may be 1×10^8 dyne/cm^2.

By isolating a 1-cm square of the layer as a free body, shown in Fig. 2, we determine from the equilibrium of vertical forces

$$\delta_m = \frac{\sigma}{\rho g} . \qquad (1)$$

For $\sigma = 1 \times 10^8$ dyne/cm^2, $\rho = 0.50$ g/cm^3, and $g = 981$ cm/s^2, we obtain $\delta_m = 2.04 \times 10^5$ cm, which is at least 10^5 times greater than required. Clearly, an adhering film of liquid lithium will be destroyed by instabilities and not by its inability to support itself. A stability analysis will have to take into account the dynamic response and surface tension of lithium. Such an investigation is beyond the scope of the present report in which only the steady-state flow is being determined.

B. Governing Equations

The steady-state flow of liquid lithium in a film of thickness δ on the inside of a sphere of radius R, as shown in Fig. 1, must conserve momentum and mass. To express these conditions in mathematical form, we consider a control volume shown in Fig. 1 and use the standard derivation technique of fluid mechanics. The assumption of uniform pressure inside the reaction cavity eliminates the pressure gradient in the layer (incompressible liquid) and leaves only inertia, gravity, and viscous forces to be considered. Their balance in the tangential direction yields

$$2\rho v \frac{dv}{d\theta} A_t \, d\theta + \rho v^2 \frac{d A_t}{d\theta} d\theta = \rho g \frac{dh}{d\theta} A_t \, d\theta - \frac{2\mu}{(0.1\delta)^2} v A_n \delta , \qquad (2)$$

where v is the tangential velocity in the θ direction, μ is the viscosity, and A_t and A_n are the cross-sectional areas perpendicular to the tangential and normal directions. The second term on the left-hand side is the geometric effect due to diverging ($\theta < \pi/2$) and converging ($\theta > \pi/2$) streamlines, and the second term on the right-hand side is the viscous drag force calculated by assuming that the flow will contain a laminar sublayer of thickness 0.1δ in which the velocity distribution will be parabolic. The consistency of this assumption will be determined from the values of Reynolds number of the resulting flow.

Substituting into Eq. (2) the expressions for the geometric factors

$$h = R(1 - \cos \theta), \qquad (3)$$

$$A_t = R \sin \theta \, d\phi \, \delta, \qquad (4)$$

$$A_n = R^2 \sin \theta \, d\theta \, d\phi , \qquad (5)$$

where ϕ denotes the angle about the vertical axis, we obtain

$$\frac{\rho v}{R} \frac{dv}{d\theta} + \frac{1}{2} \frac{\rho v^2}{R} \left(\frac{\cos \theta}{\sin \theta} + \frac{d}{d\theta} \ell n \, \delta \right) = \frac{1}{2} \rho g \sin \theta - 100 \frac{\mu v}{\delta^2} . \qquad (6)$$

Similarly, from the condition of mass conservation we obtain

$$m A_n = \rho \frac{dv}{d\theta} d\theta \, A_t + \rho v \frac{d A_t}{d\theta} d\theta , \qquad (7)$$

where

$$m = m_s - m_{ev} \tag{8}$$

is the difference between mass supplied through the porous wall, $m_s(\theta)$, and that evaporated at the free surface, m_{ev}, in $g/cm^2 \cdot s$. Substitution of the proper geometric factors transforms Eq. (7) into

$$\rho \frac{dv}{d\theta} + \rho v \left(\frac{\cos \theta}{\sin \theta} + \frac{d}{d\theta} \ell n \, \delta \right) = \frac{R}{\delta} m \ . \tag{9}$$

With the aid of some algebra, Eqs. (6) and (9) are simplified into the form suitable for numerical integration,

$$\frac{dv}{d\theta} = gR \frac{\sin \theta}{v} - \frac{200 \, R\mu}{\rho \delta^2} - \frac{Rm}{\rho \delta} \ , \tag{10}$$

$$\frac{dZ}{d\theta} = \frac{Rm}{\rho} - \delta \cos \theta \frac{v}{\sin \theta} \ , \tag{11}$$

$$Z = v\delta \ . \tag{12}$$

C. Behavior at $\theta=0$ and Initial Conditions

Clearly, Eqs. (10) and (11) are singular at $\theta=0$ and this singularity must be disposed of before the equations can be integrated. Towards this end, we observe from flow symmetry that the initial condition

$$v = 0 \text{ at } \theta = 0 \tag{13}$$

must hold, and that the apparently singular term $v/\sin \theta$ is therefore indeterminate; it can be evaluated by using L'Hospital's rule to yield

$$\lim_{\theta \to 0} \frac{v}{\sin \theta} = \frac{dv}{d\theta} \ . \tag{14}$$

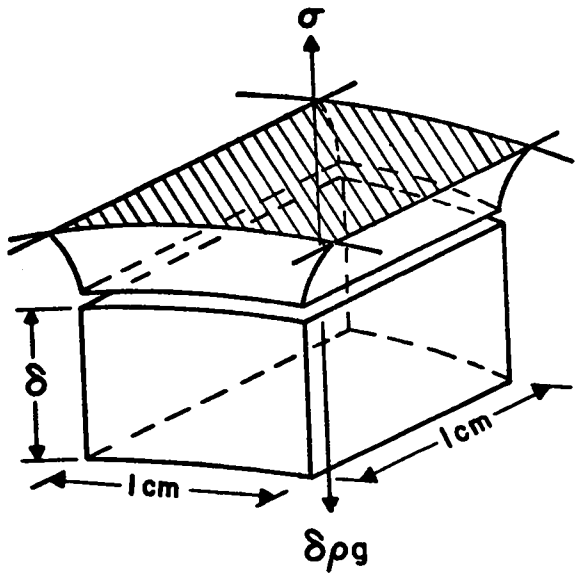

Fig. 2.
Adhesive and cohesive support of a liquid film.

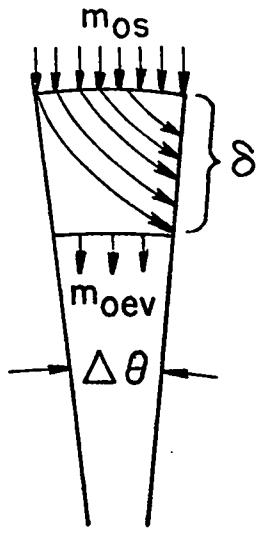

Fig. 3.
Mass flux at the origin.

Substituting Eq. (14) into Eqs. (10) and (11), solving the resulting quadratic equation, and choosing the positive square root for physical reasons, we obtain the pair of equations valid at $\theta=0$,

$$\frac{dv}{d\theta} = \frac{R}{\rho\delta_o}\left\{-\left(\frac{m_o}{2} + \frac{100\ \mu}{\delta_o}\right) + \left[\left(\frac{m_o}{2} + \frac{100\ \mu}{\delta_o}\right)^2 + \frac{g\rho^2\delta_o^2}{R}\right]^{1/2}\right\} \qquad (15)$$

$$\frac{dZ}{d\theta} = \frac{Rm_o}{\rho} - \delta_o \frac{dv}{d\theta}\ , \qquad (16)$$

where the subscript o denotes quantities evaluated at $\theta = 0$.

To determine the initial condition for δ, i.e., δ_o, we consider the mass flux in a $\Delta\theta$ neighborhood of $\theta=0$ as shown in Fig. 3. Using the expansions

$$\delta = \delta_o + \delta_1\Delta\theta + \ldots\ ,$$

$$v = \frac{dv}{d\theta}\Big|_o \Delta\theta + \ldots\ ,$$

$$\delta v = \delta_o \left.\frac{dv}{d\theta}\right|_o \Delta\theta + \ldots$$

to express the conservation-of-mass condition

$$2\pi \int_0^{\Delta\theta} m\, R \sin\theta\, R\, d\theta = 2\pi R \sin\Delta\theta\, \delta\rho v\big|_{\Delta\theta} \tag{17}$$

accurately to within linear terms in $\Delta\theta$, we obtain

$$\left.\frac{dv}{d\theta}\right|_o = \frac{1}{2} R \frac{m_o}{\rho\delta_o} . \tag{18}$$

This value of $dv/d\theta$ is independent of Eq. (15) (because one expresses conservation of mass, the other conservation of momentum) and is not identical with it (because it does not contain gravitational acceleration g). However, for consistency, the two expressions for $dv/d\theta$ must be equal; and that equality is a relationship between δ_o and m_o

$$\frac{3}{4} m_o^2 + \frac{100\, m_o\, \mu}{\delta_o} - \frac{g\rho^2 \delta_o^2}{R} = 0, \tag{19}$$

which, when solved for δ_o, provides the initial condition for Eqs. (15) and (16). Thus the formulation is complete. In practice, Eq. (19) may be used either to determine δ_o when m_o is specified or to determine m_o when δ_o is prescribed.

D. Integration

Equations (10), (11), (12) with initial relations (15), (16) and initial conditions (13), (19) constitute a well-posed initial value problem for two nonlinear, ordinary differential equations. To obtain a solution, they are integrated numerically from $\theta=0$ to some value $\theta_m < \pi$, thus avoiding the second singularity at $\theta=\pi$. This restriction does not constitute any loss of realism because

the neighborhood of $\theta=\pi$ is taken up by an opening in the cavity necessary to drain liquid lithium and evacuate gaseous reaction products.

Before integration can proceed, we must specify the mass-supply function $m_s(\theta)$. We used two forms for $m_s(\theta)$ in our investigation.

a. $m_s(\theta) = m_{os}(\text{const})\ 0 \leq \theta \leq \theta_f \leq \theta_m$

$= 0,\ \theta_f < \theta \leq \theta_m$

b. $m_s(\theta)$ decreasing linearly from m_{os} at $\theta=0$ to 0 at $\theta = \theta_f \leq \theta_m$.

For m_{ev} we used a constant

$$m_{ev} = \frac{E_{ev} P_{rr}}{4\pi R^2 H_v} \ (g/cm^2 \cdot s) \ , \tag{20}$$

where E_{ev} is the energy absorbed in the liquid layer per pulse (i.e., microexplosion), P_{rr} is the pulse repetition rate, and H_v is the heat of vaporization.

A test for accuracy of the integration scheme can be derived from the mass-conservation condition at $\theta=\theta_m$; it is

$$\delta v|_{\theta_m} = \frac{R\int_0^{\theta_f} m(\theta) \sin\theta \, d\theta}{\rho \sin\theta_m} \ . \tag{21}$$

In all computations, condition (21) was satisfied within four significant figures.

III. RESULTS

Results have been calculated for the following set of parameters:

$$\left.\begin{aligned} R &= 150 \text{ cm} \\ H_v &= 21.5 \times 10^3 \text{ J/g} \\ E_{ev} &= 22.1 \times 10^6 \text{ J/pulse} \\ P_{rr} &= 1 \end{aligned}\right\} \ m_{ev} = 3.64 \times 10^{-3} \ g/cm^2 \cdot s$$

$\mu = 4.5 \times 10^{-3}$ dyne·s/cm^2

$\rho = 0.50$ g/cm^3

To facilitate comparison among different solutions, m_{os} in each case was determined in such a way that the mass flow of lithium across the porous wall, integrated over the sphere, was 2000 g/s. Equation (19) was then used to calculate the appropriate initial condition δ_o. In all solutions $\theta_m = 15\pi/16$.

A. Uniform Mass Supply

For $m_s(\theta)$ represented by a step function $m_s(\theta) = m_{os}$, $0 \leq \theta \leq \theta_f$; $m_s(\theta) = 0$, $\theta_f < \theta \leq \theta_m$, three cases were computed corresponding to $\theta_f = 1\pi/2$, $3\pi/4$, and $15\pi/16$. The results presented graphically in Fig. 4 show that, as expected, the lithium layer becomes thinner and more nearly uniform as the supply is spread over larger portions of the spherical surface. In all cases, the thickness δ builds up rapidly towards the bottom of the reactor cavity.

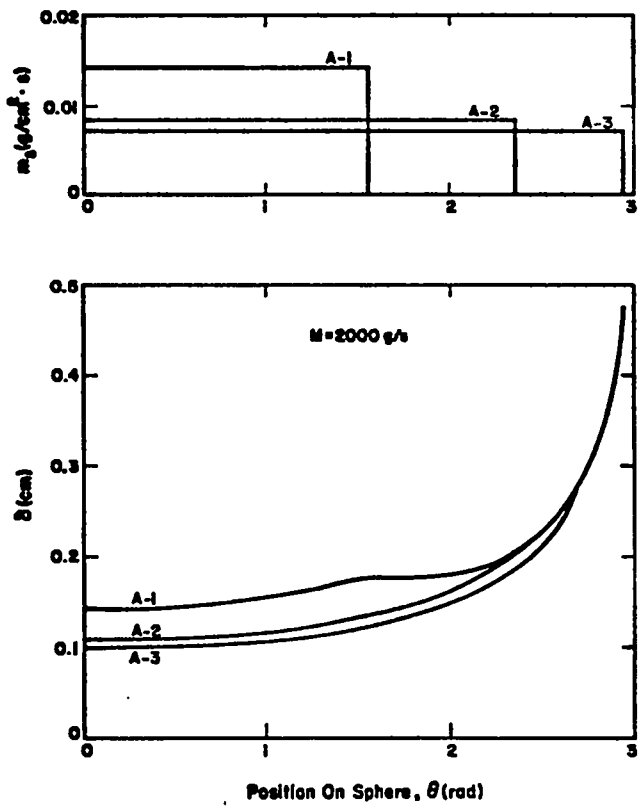

Fig. 4.
Lithium layer thickness.

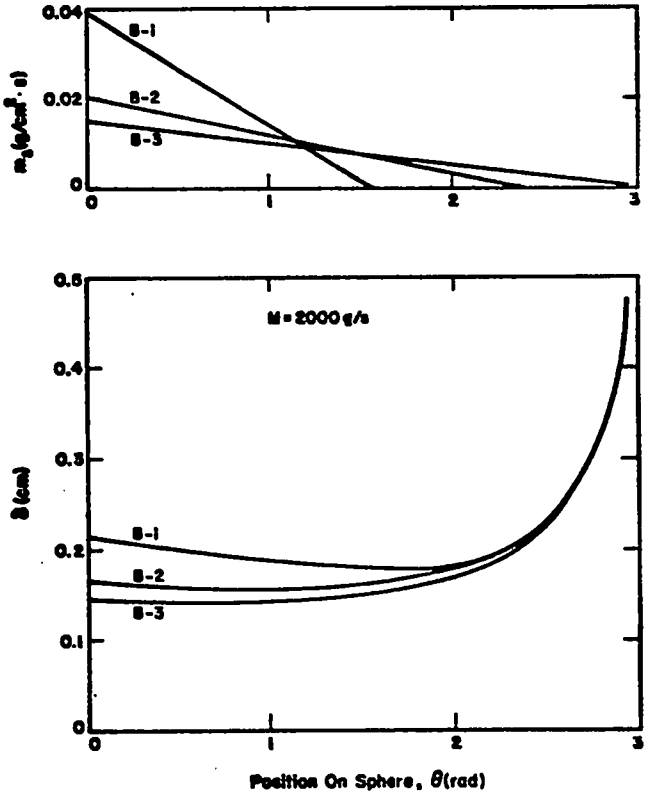

Fig. 5.
Lithium layer thickness.

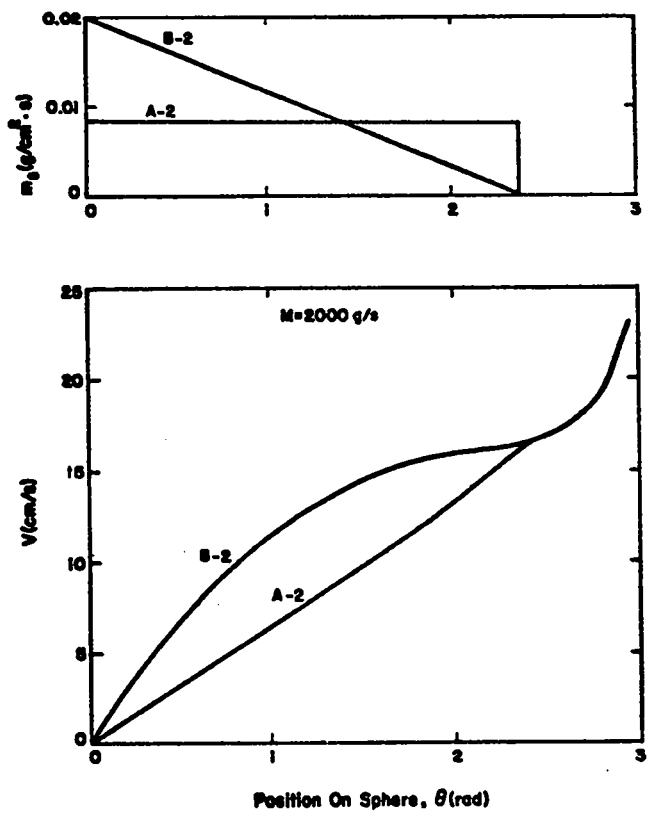

Fig. 6.
Flow velocity.

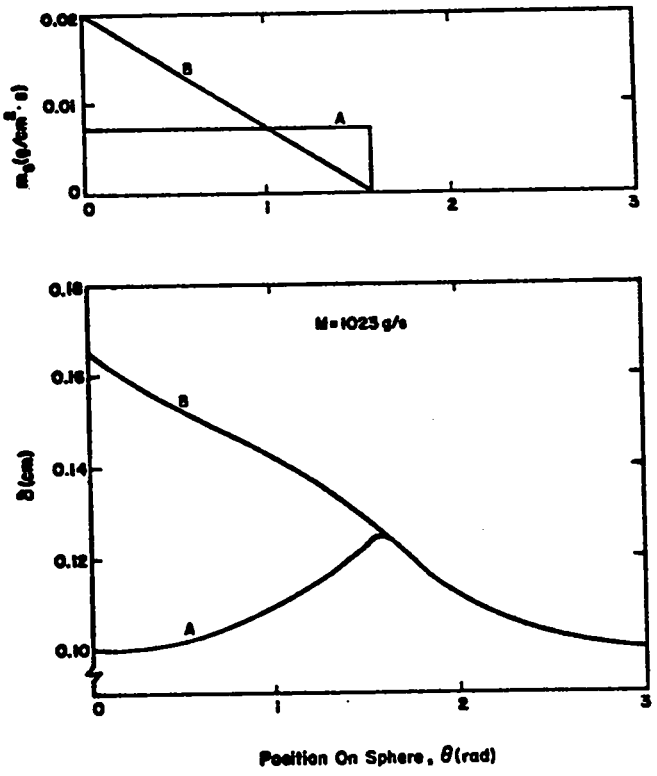

Fig. 7.
Layer thickness for mass supplied equal to mass evaporated.

B. Linear Mass Supply

The cases when $m_s(\theta)$ decreases linearly from maximum value m_{os} at $\theta=0$ to 0 at $\theta=\theta_f$ are shown in Fig. 5 for $\theta_f = 1\pi/2$, $3\pi/4$, and $15\pi/16$. Again the thickness δ decreases and becomes more nearly uniform as the mass supply is spread over a larger portion of the sphere. When m_s decreases steeply, i.e., when most of the mass is supplied near the top, $\theta=0$, the layer is thicker at the top than in the middle of the sphere.

The velocities corresponding to step and linear functions $m_s(\theta)$ are shown in Fig. 6. The values increase monotonically with θ and the magnitudes are moderate.

C. Special Solutions

Of particular interest are solutions that are obtained when the total mass supplied equals that evaporated, which is 1023 g/s for the conditions listed at the beginning of this section. Shown in Fig. 7 are the thickness distributions δ for uniform (A) and linearly decreasing (B) mass supplies over the top hemisphere. For uniform supply, the layer thickens by 25% towards the equator and

then thins down to its original value. For linearly decreasing supply, the thickness decreases monotonically, but remains greater than 1 mm.

Figure 8 shows the layer thickness and flow velocity when the same mass, 1023 g/s, is distributed linearly over the entire sphere. In this case the layer thickness δ has a minimum near the equator, $\theta=\pi/2$, which corresponds to the velocity maximum.

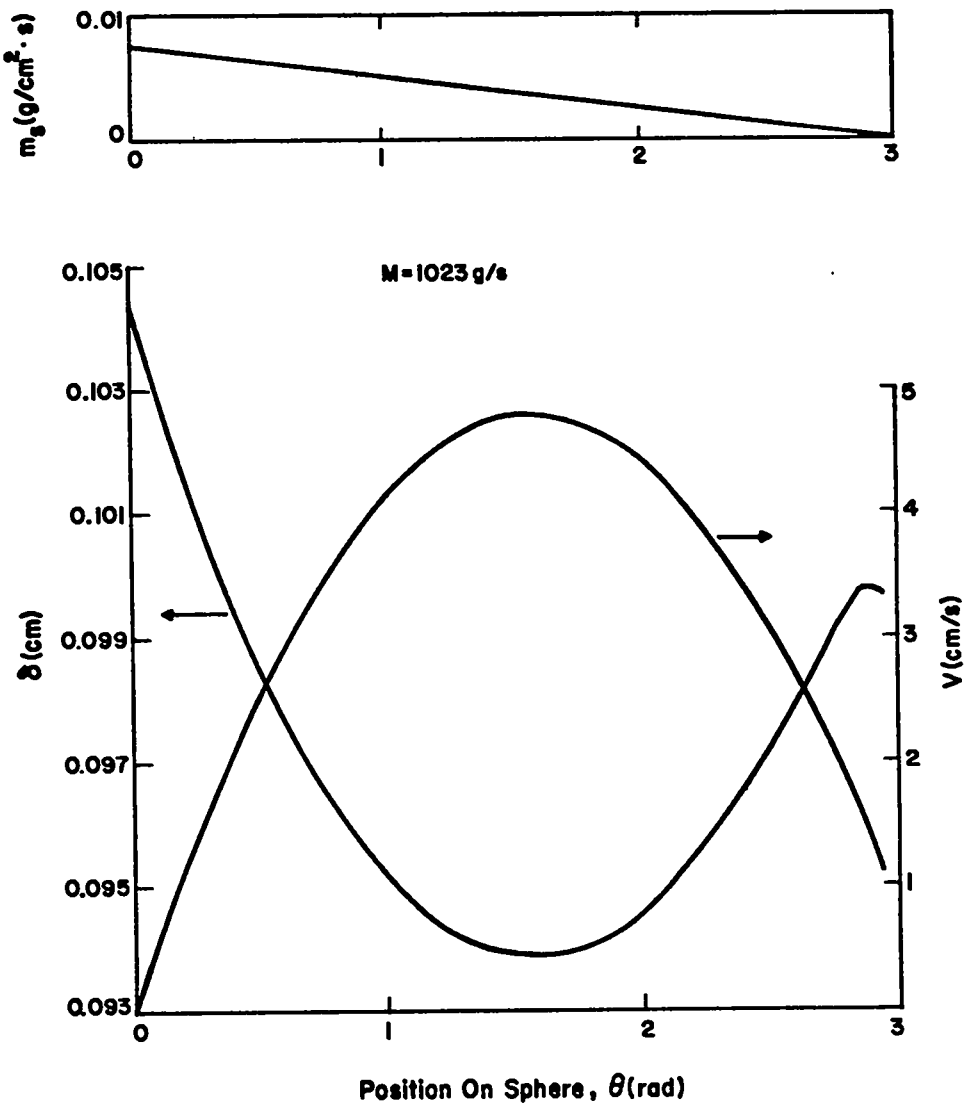

Fig. 8.
Layer thickness and velocity for mass supplied equal to mass evaporated.

D. Self-Consistency of the Model

To demonstrate the consistency of the model with calculated flows, we show that the velocity through the porous wall is sufficiently low to resemble diffusion and the Reynolds number is sufficiently high to make the flow turbulent; these two properties justify one-dimensional approximation.

The velocity through the porous wall will be highest when m_{os} is largest; in our computations this value of m_{os} is 0.04 $g/cm^2 \cdot s$. The corresponding velocity is given by $v_{pw} = m_{os}/\rho = 0.08$ cm/s, which is small indeed in comparison with typical tangential velocities presented in Fig. 6.

Using 15 cm/s as a representative maximum velocity (Fig. 6), the Reynolds number based on the radius of the spherical cavity is 250,000. This value is sufficiently high to ensure turbulent flow with uniform velocity except for a laminar sublayer. Thus, the results are consistent with the hypothesis implicit in the formulation of the problem.

IV. CONCLUDING REMARKS

The model of liquid-lithium film on the inside of a spherical reactor cavity and results obtained with it demonstrate that such steady state flows can be easily sustained. Thus, the present analysis confirms qualitatively the preliminary findings reported in Ref. 1 which were part of the basis for the wetted-wall reactor concept. The results also indicate that with a judicious choice of the mass supply function $m_s(\theta)$, the liquid thickness δ can be shaped to have a maximum either at the top or in the middle of the sphere; a second maximum will occur most of the times at the bottom.

The calculated average representative flow velocities are approximately 10 cm/s and therefore the average residence time for a parcel of lithium will be approximately 47.1 s. Thus, if a steady-state flow as determined in this investigation persisted, the same parcel would be subjected to numerous microexplosions. The transient behavior and stability of lithium film under mechanical and thermal loadings imposed by repeated pulses remain to be determined.

Another type of stability analysis may be required because the flow is in the turbulent regime (Re = 250,000). Turbulence in the liquid layer could generate surface ripples which could grow into droplets and separate from the main flow. Such a phenomenon appears unlikely because of the high surface tension of liquid lithium ($\sim$ 380 dynes/cm[5,6]), however, it should be investigated.

In the above indicated transient and stability analyses, two-dimensionality of the flow and surface-tension effects will have to be included, and, therefore, numerical modeling will most likely be required.

REFERENCES

1. L. A. Booth, Compiler, "Central Station Power Generation by Laser-Driven Fusion," Los Alamos Scientific Laboratory report LA-4858-MS Vol. I (February 1972).
2. J. M. Williams, T. Merson, F. T. Finch, F. P. Schilling, and T. G. Frank, "A Conceptual Laser Controlled Thermonuclear Reactor Power Plant," Proc. 1st Topical Meeting on the Technology of Controlled Nuclear Fusion, San Diego, CA, Vol. I, (1974), p. 70.
3. T. Frank, D. Freiwald, T. Merson, and J. Devaney, "A Laser Fusion Reactor Concept Utilizing Magnetic Fields for Cavity Wall Protection," Proc. 1st Topical Meeting on the Technology of Controlled Nuclear Fusion, San Diego, CA, Vol. I (1974) p. 83.
4. J. M. Williams, F. T. Finch, T. G. Frank, and J. S. Gilbert, "Engineering Design Considerations for Laser Controlled Thermonuclear Reactors," Proc. 5th Symp. on Engineering Problems of Fusion Research, Princeton, NJ (1973) p. 102.
5. J. O. Cowles and A. D. Pasternak, "Lithium Properties Related to Use as a Nuclear Reactor Coolant," Lawrence Radiation Laboratory report UCRL-50647 (April 1969).
6. P. Y. Achener, "Alkali Metals Evaluation Program: Surface Tension and Contact Angle of Lithium and Sodium," Aerojet-General Corp. report AGN-8191, Vol. 3 (April 1969).
7. D. O. Jordan and J. E. Lane, "The Wetting of Solid Metals by Liquid Alkali Metals," in The Alkali Metals (Chem. Soc. of London, Spec. Publ. 22, 1967), p. 147.
8. W. L. Nyborg, A. F. Scott, and F. D. Ayres, "Tensile Strength and Surface Tension in Liquids," in American Institute of Physics Handbook, 3rd Edition (McGraw-Hill, New York, 1972) p. 2-202.